Placozoan microbiomes reveal evolutionary trajectories towards mutualism among the largely parasitic *Rickettsiales*

Anna Mankowski[1,2*], Henry Berndt[3], Nikolaus Leisch[1,4], Hiroaki Nakano[5], Genichiro Nishi[5], Michael G. Hadfield[6], Bruno Hüttel[7], Tina Enders[1], Nicole Dubilier[1], Harald R. Gruber-Vodicka[1,3*]

[1]Max Planck Institute for Marine Microbiology, Bremen Germany
[2]Molecular Systems Biology Unit, European Molecular Biology Laboratory, Heidelberg, Germany
[3]Zoological Institute, Christian-Albrechts-Universität zu Kiel, Kiel, Germany
[4]Mobile Laboratories Facility, European Molecular Biology Laboratory, Heidelberg, Germany
[5]Shimoda Marine Research Center, University of Tsukuba, Shimoda, Shizuoka, Japan
[6]Kewalo Marine Laboratory, Pacific Biosciences Research Centre, University of Hawai'i at Mānoa, Honolulu, HI, USA
[7]Max Planck Genome Centre Cologne, Max Planck Institute for Plant Breeding Research, Cologne, Germany

* Corresponding authors:
Anna Mankowski: anna.mankowski@embl.de
Harald R. Gruber-Vodicka: hgrubervodicka@zoologie.uni-kiel.de

Abstract

Rickettsiales are an enigmatic clade of strictly host-associated bacteria with some very common phylotypes in aquatic habitats. Despite amplicon- and metagenomic sequencing-based observations, the roles of these aquatic *Rickettsiales* are still unknown, as their genomes feature both beneficial and parasitic traits. In placozoans, microscopy-based observations of intracellular and *Rickettsia*-like-organisms point to *Rickettsiales* as common and abundant symbionts. We therefore systematically studied the microbiomes of placozoans to understand the eco-evolutionary dynamics of their associated *Rickettsiales*. Single-animal metagenomics revealed a widespread association of placozoans with *Rickettsiales* from three clades of '*Ca.* Midichloriaceae', which were present in all but two placozoan lineages. A comparative phylogenetic analysis of placozoans and their *Rickettsiales* symbionts revealed host species-specific switches among *Rickettsiales* clades in several placozoan lineages. Our combination of evolutionary analyses, genome annotations, and expression data indicate different functional roles of these *Rickettsiales* clades, with some clearly diverging from a classical parasitic lifestyle by the loss of all ATP scavenging machinery. One of placozoan lineages that lacked '*Ca.* Midichloriaceae' was instead associated with *Rickettsiaceae* symbionts, while another was completely devoid of *Rickettsiales* symbionts. Our imaging data of fibre cells entirely free of *Rickettsiales* underscores previously unrecognized variation in placozoan–microbe associations. Early-branching invertebrates, including placozoans as well as many corals, are gaining increasing traction as emerging models across the life sciences. Our data and analyses show that it is important to consider the specific endosymbiont groups and their ecology in a given host, as these symbionts likely influence the hosts' cellular and organismal biology.

Introduction

Several clades of bacteria are fully adapted to a host-dependent lifestyle, with all known members characterized exclusively as symbionts of other organisms. One of these enigmatic clades is the order *Rickettsiales*, alphaproteobacterial symbionts that occur intracellularly across a wide range of eukaryotic hosts, including many animals. They are generally regarded as parasites and cause a variety of diseases in humans, livestock and wild animals (*1, 2*). Although *Rickettsiales* are well characterized from terrestrial systems and insect hosts, their associations with marine invertebrates and protists have received comparatively less attention.

A key host group of marine *Rickettsiales* are placozoans, a phylum of globally distributed, benthic invertebrates that emerged very early in animal phylogeny (*3–5*). With their simple, two-layered bauplan and limited obvious morphological differentiation, placozoans were long considered a monotypic 'phylum-of-one'. Molecular taxonomic studies first using mitochondrial 16S rRNA genes (haplotypes) and later comparative genomic analyses of placozoan genomes, alongside diversity patterns in other early-branching metazoans such as Cnidaria and sponges, have recognized four

placozoan orders and six families. These include four formally described genera (*Trichoplax*, *Hoilungia*, *Polyplacotoma*, and *Cladtertia*) and three putative genera not yet formally described. The analyses of mitochondrial haplotypes indicated a large diversity of cryptic species (haplotypes) that are morphologically indistinguishable within placozoan genera (*3, 6–8*). Microscopy studies have consistently revealed that all placozoans examined harbor intracellular bacteria inside the fiber cells endoplasmic reticulum (*6, 9–11*). This widespread association between placozoans and intracellular bacteria, initially described from microscopy data, was also corroborated with genomic data in two placozoan lineages, and together with correlative light- and electron microscopy data indicates that these symbionts are *Rickettsiales* (*6, 9, 11–14*). This genomic data and symbiont specific imaging data for associated *Rickettsiales* so far came from two of the most closely related placozoan lineages from the genus *Trichoplax* (*14, 15*). In *Trichoplax adhaerens* (H1) and *Trichoplax* sp. 'H2', two closely related *Rickettsiales* genera from the family 'Ca. Midichloriaceae', 'Ca. Grellia' and 'Ca. Aquarickettsia' (*Midichloriaceae*, *Grellia* and *Aquarickettsia* from here on) were identified (*6, 13, 14*). However, the nature of the association between these two *Midichloriaceae* symbiont lineages and their placozoan hosts remains elusive, as their genomes appear to contain both mutualistic and parasitic traits (*14, 16*).

In this study, we analyzed the microbiomes of placozoans with an emphasis on putatively intracellular symbionts and specifically *Rickettsiales* by systematically sampling 115 single-animal metagenomes across the phylum Placozoa from nine sampling sites, representing three of the four orders of placozoans (*3, 17*). We combined a reconstruction of the host phylogeny with a systematic profiling of the microbiome of each individual, using primer-free and metagenome-based reconstruction of full-length host mitochondrial and bacterial 16S rRNA genes. We then focused on the *Rickettsiales* symbionts, analyzed their phylogenetic relations as well as their distribution across host haplotypes and performed last common ancestor reconstructions to recapitulate the evolutionary history between placozoans and *Rickettsiales* symbionts. We found an unexpected diversity with four different clades of *Rickettsiales* symbionts linked to host haplotypes, with host population specific association patterns across sites.

Results & Discussion

Placozoans are associated with a large diversity of putative symbionts

To describe the microbiome of placozoans across a broad biogeographic host range, we used single animal DNA extractions to generate ultra-low input shotgun DNA libraries from 115 host individuals from eight host mitochondrial 16S rRNA genotypes (host haplotypes) sampled in nine globally distributed locations (Fig. 1A-D, Table S1). We identified host haplotypes by reconstructing full-length mitochondrial 16S rRNA gene sequences, the standard in placozoan molecular taxonomy, and by inferring phylogenetic relationships between our samples and reference sequences (Figure 1D, Figure 2) (*3*). To characterize host-associated microbiomes, we first generated a database of *de novo* assembled 16S rRNA sequence from all metagenomes. Reconstructed sequences were summarized at the family level, except for *Rickettsiales*, which were split into genus-level taxa due to our specific research focus (Table S2). This database was then used for reference-based sequence reconstruction and to estimate the relative abundance of each taxon in individual hosts. Potential chimeras, likely human- or flow-cell–derived contaminants, and singleton families were removed, and relative abundances were normalized for downstream analyses (Note S1).

Our microbiome screening revealed a widespread and consistent association of placozoans with *Rickettsiales* symbionts (Fig. 1), including phylotypes that belong to the previously described *Grellia* and *Aquarickettsia* clades (*13, 14, 18*). The screening of many different haplotypes and sampling sites however revealed an even larger diversity of placozoan-associated *Rickettsiales*. In total, we detected five genera specifically associated with different haplotypes from different sampling locations (Fig. 1,

105 Fig. 2). In addition, we detected intracellular bacteria from the *Margulisbacteria*, '*Ca*. Ruthmannia'
106 (*Ruthmannia* from here on) in three placozoan haplotypes from four locations (Fig. S1D). *Ruthmannia*
107 symbionts have been previously characterized with genomic, expression and microscopy data in the H2
108 haplotype (*14*). Their association with placozoans appears patchy but more common than
109 anticipated (*19*), as they were repeatedly present across haplotypes and sampling sites. We
110 additionally detected three more families of putative endosymbionts which have not been described as
111 placozoan symbionts yet. These include two clades of *Simkaniaceae* (Fig. S1A) and one clade of
112 *Coxiellaceae* (Fig. S1B), both known to occur solely as intracellular symbionts of diverse eukaryotes (*20,*
113 *21*). In addition, we detected one clade of *Endozoicomonadaceae* (Fig. S1C), a family of common
114 symbionts of marine invertebrates (*22–24*). The *Endozoicomonadaceae* detected in placozoans are only
115 distantly related to the well-characterized genus *Endozoicomonas* and represent a new genus we name
116 '*Ca*. Endoplacomonas' (*Endoplacomonas* from here). While there is a high chance that these three
117 families are yet uncharacterized endosymbionts of placozoans, their position in the animals and their
118 roles still needs genomic reconstructions and microscopy-based detection, e.g., via fluorescence *in situ*
119 hybridization using taxon-specific probes.
120 Beyond the detection of five families of putative endosymbionts, we detected 24 additional families.
121 23 of these 24 families had a broad geographic or taxonomic range of hosts, but occurred only in a
122 few individuals, which might indicate a non-specific association, sequencing bias or contamination, e.g.,
123 members of the *Flavobacteriaceae*. In contrast, the *Teraskiellaceae (Alphaproteobacteria*) were only
124 detected in certain haplotypes (H3, H6, H7 and H8), but consistently across all specimens, which could
125 indicate a specific association. However, further investigation and additional data are necessary to
126 understand the nature of their relationships to placozoans.

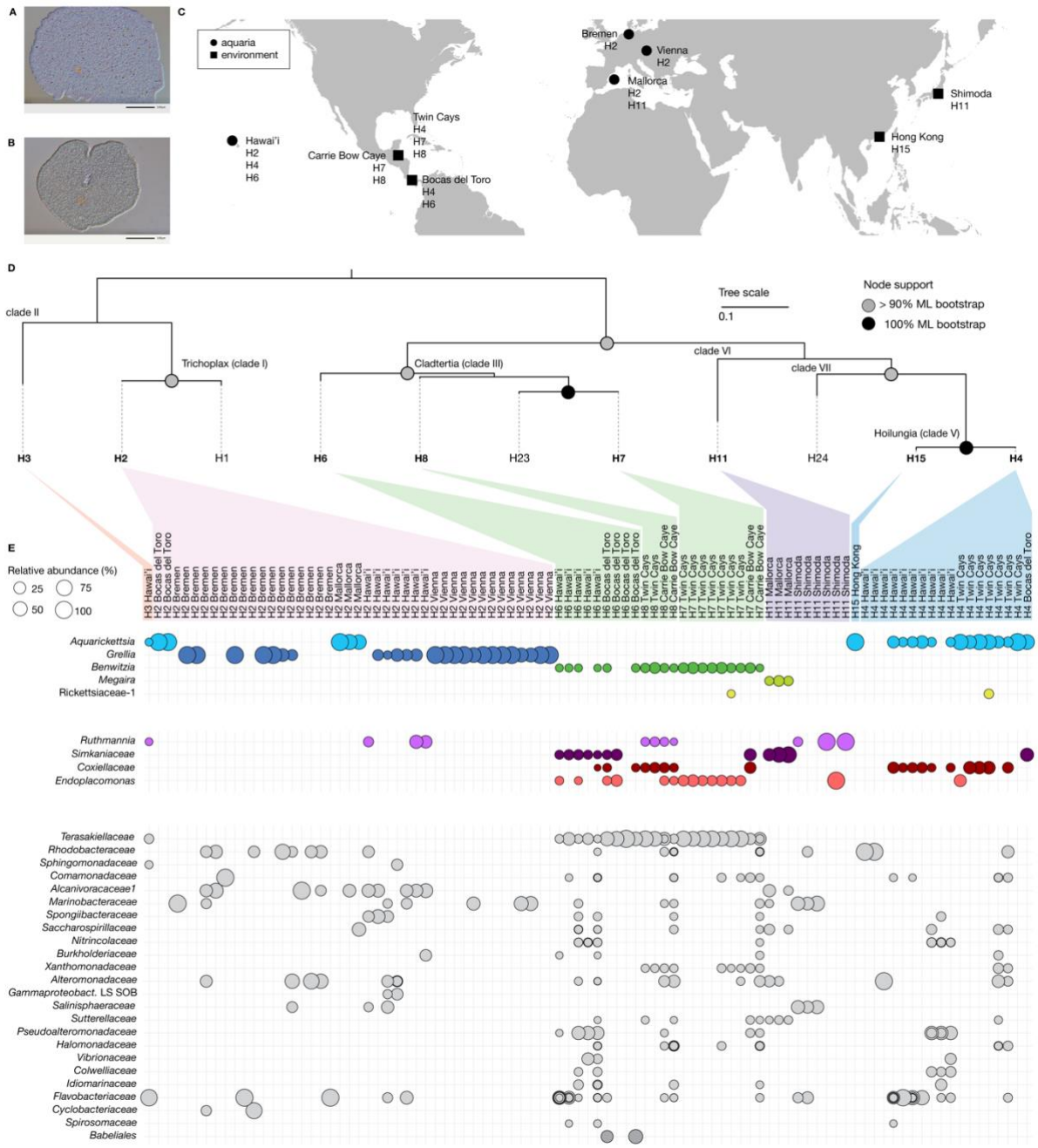

Figure 1 | Placozoan individuals are associated with diverse microbiomes. A: DIC micrographs of a *Trichoplax* sp. H2 sampled in Vienna, Austria. B: DIC micrograph of a placozoan H11 sampled in Shimoda, Japan. C: World map showing sampling sites and detected host haplotypes. Circles indicate samples from aquaria, squares samples from the natural environment. D: Maximum-likelihood trees of the host mitochondrial 16S rRNA gene using one individual per host haplotype, with haplotypes analyzed in this study highlighted in bold. The scale bar indicates 10% estimated sequence divergence. Nodes with bootstrap support > 90% are shown in grey and 100% support in black. E: Relative abundances of all associated bacteria per host individual, as estimated with EMIRGE based on full-length 16S rRNA sequences from metagenomes. Each column represents a single host individual, and each row lists the identified bacterial group to the left, and shows abundances as dot plots scaled by relative abundance. Rows are arranged to show intracellular taxa on top, starting with members of the *Midichloriaceae*. Note that almost all host individuals have detectable amounts of *Rickettsiales* endosymbionts, largely *Midichloriaceae*. Most other bacterial families are irregularly distributed, and are often restricted to specific host clades, e.g. the *Endoplacomonas*. *Rickettsiales* symbionts are colored by genus; other putative endosymbionts are colored by class; all other detected bacteria are shown in gray.

143 Our microbiome characterization revealed a so far undescribed diversity of bacteria associated with
144 placozoans, in varying degrees of specificity across host haplotypes and sampling sites. For many of
145 them, the type of association as well as their role and impact on placozoans remains unclear, but, given
146 their phylogenetic background, five of the detected families are very likely intracellular
147 endosymbionts. While most bacterial representatives were associated with a few
148 individuals/haplotypes, the association with *Rickettsiales* symbionts is almost omnipresent across the
149 diversity of placozoan hosts. We only detected a single lineage (H11 from Shimoda, Japan) in which
150 none of the specimens was associated with *Rickettsiales* symbionts (Figure 1, Table S3). In all other
151 lineages, we detected *Rickettsiales* in at least a subset of the specimens. For many specimens in which
152 we could not assemble a full-length 16S rRNA gene, we nevertheless detected medium to high
153 proportions of reads mapping to *Rickettsiales* reference genomes (Table S3). This indicates that
154 *Rickettsiales* were likely present but could not be assembled due to low sequencing coverage. In
155 addition to *Rickettsiales*, no more than two other putative endosymbiotic taxa were detected per
156 individual. It remains to be shown if they are cell-type specific and do not co-occur, as was shown for
157 *Grellia* and *Ruthmannia* in H2 (*14*), or if they overlap in certain cell types in some host-symbiont
158 combinations.
159
160 **Diversity, distribution and evolutionary history of *Rickettsiales* symbionts**
161 Given the widespread and consistent association between placozoans and *Rickettsiales*, we next
162 explored the hypothesis that the *Rickettsiales* are linked to patterns of placozoan evolution. To this end
163 we excluded the genus 'Rickettsiaceae-1' from our downstream analyses, as this phylotype was
164 detected only sporadically and in relatively low abundance, and always co-occurred with a higher
165 abundant and more broadly distributed *Rickettsiales* symbiont, in contrast to the widespread and high
166 abundance association between the placozoans and all other *Rickettsiales* phylotypes. For the
167 remaining and widespread assocations, our microbiome screening revealed four *Rickettsiales* genera.
168 This includes the previously described *Aquarickettsia* and *Grellia* symbionts. Both taxa belong to the
169 *Midichloriaceae* and are the sister clade to 'Ca. Bandiella'. In addition, we also detected two more
170 genera of *Rickettsiales* symbionts that have not been described in placozoans yet. The first one, we
171 name 'Ca. Benwitzia' (*Benwitzia* from here) and also belongs to the *Midichloriaceae*, while the fourth
172 one is a *Rickettsiaceae* from the genus 'Ca. Megaira' (*Megaira* from here). All four genera have been
173 reported from other marine protists and animals, indicating a broad distribution of *Rickettsiales* across
174 diverse marine hosts (Fig. 4)(*25–27*). Consistent with this, in our phylogenetic analyses, the *Rickettsiales*
175 symbionts detected in placozoans are closely related or even form intermixed clades with symbionts of
176 other marine invertebrates, most often corals, for which the association with *Aquarickettsia* has been
177 studied extensively (Figure 2)(*13, 18*).

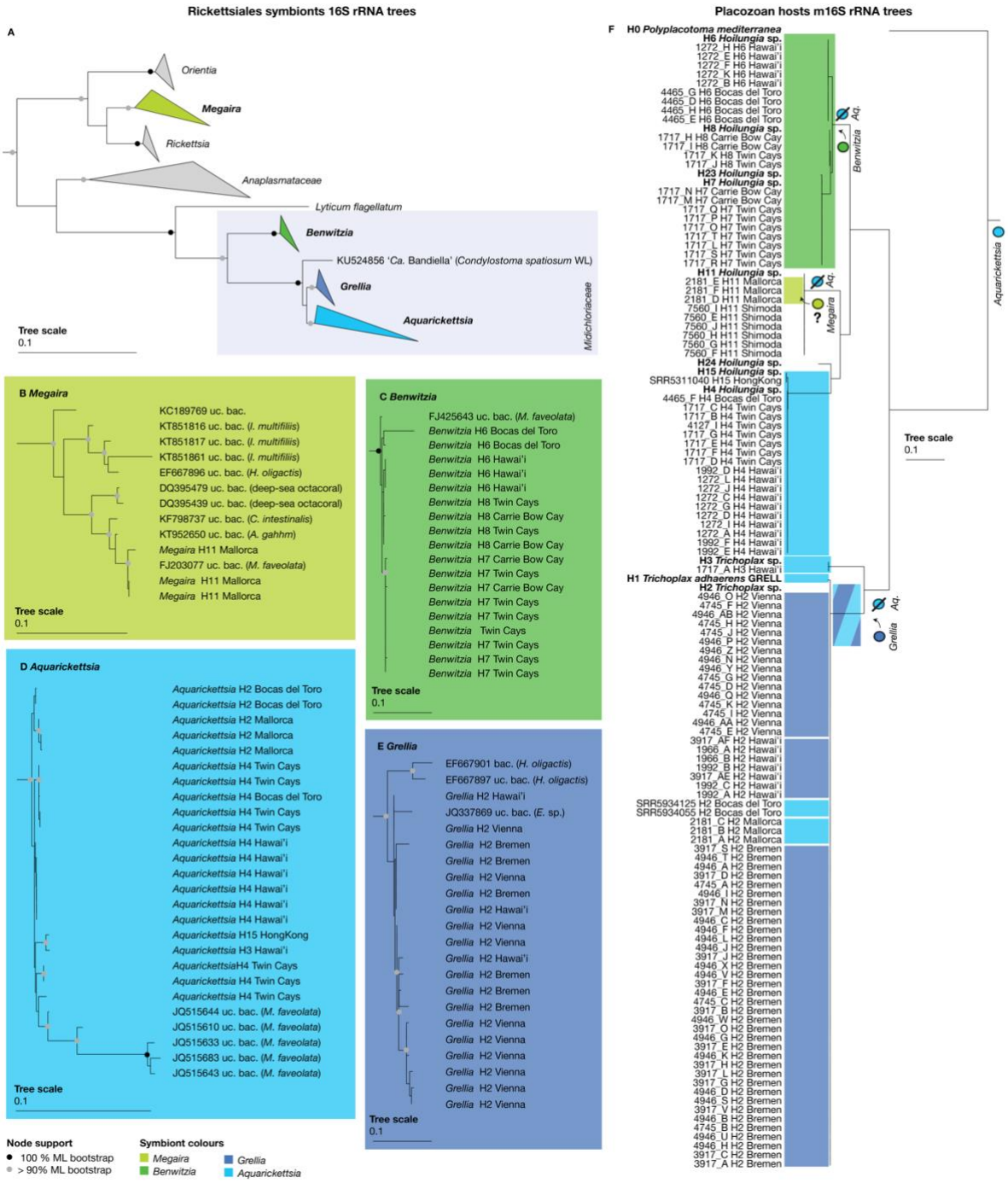

Figure 2 | Phylogeny of placozoan associated *Rickettsiales* (A-E) and their distribution and evolutionary history across the host diversity (F). A-E: 16S rRNA based phylogenetic reconstructions. A-F: scale bars indicate 10% estimated sequence divergence A: overview of the *Rickettsiales* symbionts and close relatives. Colored triangles highlight the different *Rickettsiales* symbiont genera. B: *Megaira* symbionts and close relatives. C: *Benwitzia* symbionts and close relatives. D: *Aquarickettsia* symbionts and close relatives. E: *Grellia* symbionts and close relatives. F: m16S rRNA Phylogeny of the host individuals. References are highlighted in bold. Colored boxes highlight the predicted association with the different *Rickettsiales* symbiont clades based on a maximum-parsimony model. Predicted events of symbiont losses and acquisitions are indicated at the corresponding nodes of the host phylogeny. Small cartoons illustrate the inferred symbiont lineages associated with each split based on the last common ancestor reconstruction.

We detected a *Rickettsiales* phylotype in all haplotypes from all sampling sites, except one lineage of H11 from Shimoda, Japan, and could reconstruct a full-length 16S rRNA for nearly all individuals. This widespread association between the different Rickettsiales clusters was highly specific for certain

193 haplotypes and dominated by *Midichloriaceae*, such as *Aquarickettsia* that were most widespread and
194 associated to most haplotypes (H1, H2, H3, H4 and H15). Members of *Grellia* were much rarer and
195 were only associated with lineages of the H2 haplotype from Bremen, Vienna and Hawai'i, while
196 members of the *Benwitzia* clade were found across the monophyletic clade of H6, H7 and H8
197 haplotypes. Only a single host haplotype (H11) did not host *Midichloriaceae*, but was either associated
198 with *Megaira* symbionts from the *Rickettsiaceae* (lineage from Mallorca) or did not feature any
199 *Rickettsiales* symbionts at all (isolates from Shimoda).
200
201 Our analyses indicate that *Rickettsiales* associations are ancestral in placozoans but highly dynamic,
202 with multiple independent replacement and loss events across lineages. *Aquarickettsia* appears to be
203 the primary symbiont, retained across many recent haplotypes, reflecting the ancestral state of the
204 association of placozoans with *Rickettsiales* symbionts (Table S3 and S4). In some lineages, however,
205 this symbiont has been replaced. In the *Cladtertia* clade (haplotypes H6, H7, and H8), the consistent
206 presence of *Benwitzia* across all sampled populations suggests that this symbiont replaced
207 *Aquarickettsia* in the common ancestor of the clade, and that this replacement was subsequently
208 inherited by descendant haplotypes. Similarly, in haplotype H2, three lineages (Bremen, Hawai'i, and
209 Vienna) show replacement of *Aquarickettsia* by *Grellia*, whereas populations from Bocas del Toro and
210 Mallorca retain *Aquarickettsia*. Other cases are less clear. In haplotype H11, *Aquarickettsia* is absent in
211 all specimens from Mallorca and Shimoda, and *Megaira* is present in the Mallorca population. We
212 cannot determine whether the loss of *Aquarickettsia* occurred once in a common ancestor or
213 independently in each population, nor whether the acquisition of *Megaira* preceded or followed this
214 loss. Likewise, because the host phylogeny based on mitochondrial 16S rRNA does not fully resolve
215 relationships among lineages, it is unclear whether the replacements observed in H2 populations
216 represent independent events or were inherited from a shared ancestor. Overall, these patterns
217 indicate that placozoan-*Rickettsiales* associations involve both long-term retention of ancestral
218 symbionts and repeated host-switching or replacement events, reflecting a dynamic evolutionary
219 history that remains incompletely resolved.
220
221 **H11 individuals that lack symbionts in the rough endoplasmic reticulum reveal placozoan origin**
222 **of mitochondrial complexes in fiber cells.**
223 To corroborate the symbiotic status of the *Rickettsiales*-free H11 population from Shimoda, we
224 performed differential interference contrast (DIC) microscopy on living and transmission electron
225 microscopy (TEM) on high pressure frozen specimens (Fig. 3, Fig. S2-3). Generally, the microanatomy of
226 H11 resembled the general placozoan body plan (*12*, *28–30*). In concordance with the absence of
227 any *Rickettsiales* symbionts from the metagenomic data, endosymbionts in the endoplasmic reticulum of
228 fiber cells were not observed. (Fig. 3, Note S2). The consistent presence of *Rickettsiales* in the rER of
229 fiber cells, together with the peculiar mitochondrial complexes observed in all placozoan species, led
230 to the hypothesis that these intracellular symbionts might induce the unique mitochondrial morphologies
231 that have not been reported in any other eukaryote. Here, we show that the formation of these
232 mitochondrial stacks occurs independently of *Rickettsiales*, indicating that they are an intrinsic feature of
233 the placozoan cellular bauplan (*12*).
234 Despite the absence of *Rickettsiales* symbionts in this population, we observed intracellular bacteria in
235 cells of the lower epithelium (Fig. 3C, Fig. S3J-L) and extracellular bacteria in the intra-epithelial
236 region of H11 (Fig. 3D, Fig. S3H). The identity of these bacteria remains unknown and they may be
237 food-related, loosely associated bacteria or true symbionts. Metagenomic analyses indicate that
238 *Ruthmannia* are the only abundant symbionts in all specimens from this population and morphologically,
239 the extracellular bacteria resemble the previously characterized *Ruthmannia* symbionts (*14*). This is
240 consistent with observations of *Ruthmannia* in the ventral epithelium of other Placozoa haplotypes,
241 however, in the case of H11, they seem to occur extracellularly in contrast to their intracellular
242 localization in H2 specimen (*14*). Our morphological characterization shows that H11 from Shimoda

displays the classic placozoan body plan, including distinctive mitochondrial stacks in fiber cells that appear to form independent of the presence of *Rickettsiales* symbionts.

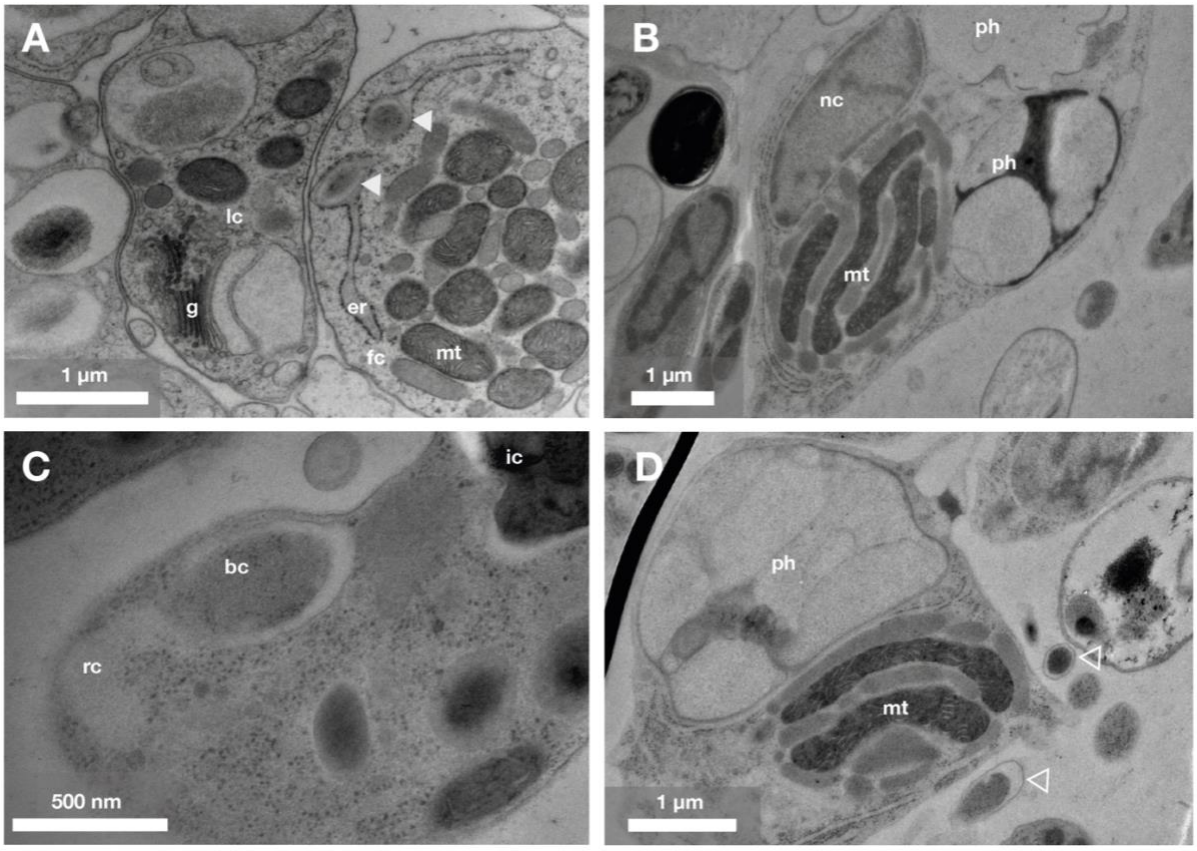

Figure 3 | The placozoan H11 from Shimoda shows the typical mitochondrial complexes in its fiber cells, but this lineage lacks the endosymbionts assumed to induce this phenotype. A: Transmission electron microscopy (TEM) micrograph of a fiber cell of *Trichoplax* sp. H2 'Vienna' containing *Grellia* in the endoplasmic reticulum (er, closed arrowheads). lc: lipophilic cell; g: golgi apparatus; mt: mitochondria. B:TEM micrograph of a fiber cell of the placozoan H11 'Shimoda' without endosymbionts in the ER. nc: nucleus; mt: mitochondria; ph: phagosome. C: TEM micrograph of an intracellular bacteria (bc) in the cytoplasm of a cell of the lower epithelium of H11. rc: reorganized cytoplasm; ic: inclusion. D: Micrograph of a fiber cell of H11 with extracellular bacteria next to it (open arrowheads). ph: phagosome; mt: mitochondria.

Genomic and transcriptomic analyses of *Rickettsiales* symbionts reveal an evolutionary trajectory to minimize the energetic burden for the host

The observation of host specificity in *Rickettsiales* symbionts led us to investigate their genomic features more closely. We therefore used metagenomic assembly and binning to generate metagenome assembled genomes (MAGs) of *Rickettsiales* symbionts from 42 samples with sufficient coverage. Symbiont genomes with sufficient quality ranged from 1.0 to 1.96 Mbp, with GC contents between 28% and 37% (for MAGs with >50% checkM2 completeness, and <10% contamination, Table S4). While these genomic traits do not indicate the extreme genome reduction seen in many insect symbionts, they nonetheless reflect a host-associated lifestyle. There was no clear trend suggesting different levels of host dependence (i.e., smaller genome size and lower GC content). Instead, genomes of *Aquarickettsia* symbionts had the lowest GC content, whereas *Grellia* genomes were the smallest. Given their close phylogenetic relationship, these subtle but stable differences in genome evolution are intriguing and points towards differences in their evolutionary trajectories. In contrast, *Megaira* genomes were the largest and had the highest GC content, with *Benwitzia* symbionts showing intermediate genome statistics.

To assess whether functional capacities differ between these symbionts, we compared the number of COG (Clusters of Orthologous Genes) categories in each genome(*31*). Despite slight differences in genome size and GC content, *Aquarickettsia* and *Grellia* were most similar among the symbiont groups based on the frequency of different COG categories and did not form distinct clusters, indicating comparable functional fingerprints. Consistent with the trends in genome size and GC content, *Megaira* was the most distinct, with *Benwitzia* falling in between (PERMANOVA: $R^2 = 0.51$, $p = 0.001$, ANOSIM: $R = 0.70$, $p = 0.001$). Although analyses of symbiont composition and evolutionary history (Figures 1 and 2) indicate that one symbiont may replace another, the observed differences in functional profiles show that these replacements do not result in complete functional equivalence.

To investigate the potential energetic burden of *Rickettsiales* symbionts on placozoan hosts, we examined their capacity for ATP parasitism. *Rickettsiales* are generally thought to scavenge ATP from their hosts via ADP/ATP translocases, while many can also generate ATP using their own ATP synthases. A genomic survey of placozoan-associated *Rickettsiales* revealed that all symbionts possess genes encoding ATP synthases, and most also carry ADP/ATP translocases (Extended Data). Notably, some *Grellia* lineages from H2 haplotypes sampled in Vienna and Bremen lack the translocase, indicating potential lineage-specific differences in ATP acquisition strategies (Extended Data, Figure S4).
To further assess functional activity, we compared expression of ATP synthase and ADP/ATP translocase genes in two *Grellia* lineages. Consistent with previous studies, only ATP synthase genes were detectably expressed, even when the translocase gene was present (*14*). These data suggest that, under the conditions examined, *Grellia* generates ATP primarily through its own synthase rather than the classical host-dependent ATP import, although occasional host-derived ATP import cannot be excluded. In contrast, *Megaira* symbionts from the H11 haplotype in Mallorca retain multiple ADP/ATP translocase variants, indicating that these symbionts rely more heavily on host ATP, consistent with a more classical parasitic strategy within the *Rickettsiaceae*. Overall, these findings highlight variation in ATP acquisition strategies among placozoan symbionts, with potential implications for the energetic burden imposed on the host, while emphasizing that functional conclusions remain tentative given the current data.

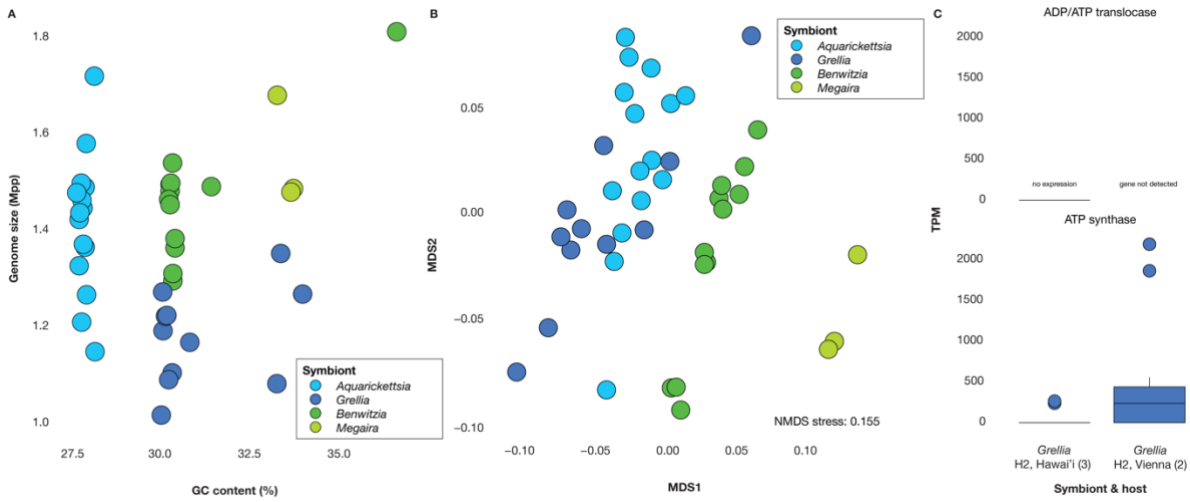

Figure 4 | Genomic and transcriptomic analyses of *Rickettsiales* symbionts indicate diverging functional profiles and a convergent loss of energy parasitism. A: Genome size (Mbp) and GC content of *Rickettsiales* genomes. Points are colored by symbiont type. B: NMDS plot of Bray-Curtis distances calculated based on the frequency of COG categories in *Rickettsiales* symbiont genomes. Points are colored by symbiont type. C: Transcription of genes for ADP/ATP translocases and ATP synthases estimated through pseudoalignment of transcriptomic reads to reference MAGs. Boxes are colored by symbiont type. Numbers in parentheses refer to the number of analyzed metatranscriptomes.

Conclusion

This study provides a detailed inventory of the placozoan microbiome, revealing both previously characterized and novel symbionts. In addition to *Rickettsiales* and *Margulisbacteria*, we identify putative endosymbiotic associations with *Endozoicomonadaceae*, *Simkaniaceae*, and *Coxiellaceae*. We also catalog a range of microbes whose association with placozoans remains uncertain. These potentially loosely associated microorganisms offer opportunities to investigate their interactions and functional roles within the host.

Among these associations, *Rickettsiales* symbionts are abundant, widespread, and specific. Our reconstructions suggest that the association with a *Rickettsiales* partner is likely ancestral across modern placozoans. Phylogenetic analyses further indicate that placozoans may exchange symbionts with other marine invertebrates, as members of all four placozoan symbiont clades are intermixed with symbionts from Cnidaria, Porifera, and Ctenophora (Figure 2) (*13, 14*). A recent study predicted that *Aquarickettsia* symbionts of corals are horizontally transmitted, suggesting a free-living life stage with likely limited survival time(*14, 16, 18*)which could provide a source for acquisition in placozoans. Given these potential symbiont switches, and the observation that both *Aquarickettsia* and *Grellia* reside in the rER lumen (*9*, *11*, *12*), placozoans may serve as a model to study how intracellular, and even intra-organelle, symbioses are established.
Despite the widespread and potentially ancient association, it remains unclear whether placozoan Rickettsiales behave as classical parasites, as observed in reef-building corals, or whether their association is more commensalistic or mutualistic. Previous genomic and transcriptomic analyses show that *Grellia* and *Aquarickettsia* genomes harbor both mutualistic and parasitic traits (*13, 14, 16*). While Rickettsiales are often described as energy parasites reliant on host ATP(*32, 33*) our analyses indicate that *Grellia* and *Aquarickettsia* symbionts appear to generate ATP primarily via their own ATP synthases, with some lineages losing ADP/ATP translocases entirely. This pattern is rare among *Rickettsiales*, previously observed only in lineages associated with protist hosts, where it has been proposed to reduce host dependence (*34*). An additional, non-exclusive possibility is that reliance on self-generated ATP minimizes energetic costs for the host. However, no comprehensive metabolic budgets are available, and the loss or absence of a translocase does not conclusively rule out occasional host ATP use. Notably, coral-associated *Aquarickettsia* often considered parasitic, also encode ATP synthases and may rely primarily on self-generated ATP, though expression has not been confirmed (*13*). Overall, these observations suggest that *Grellia* and *Aquarickettsia* diverge from classical *Rickettsiales* parasitism by reducing energetic dependence on their hosts, while the precise nature of these interactions remains unresolved. In addition, although both symbionts are auxotrophic for amino acids and nucleotides, they may supplement host diets with vitamins, such as riboflavin, which placozoans cannot synthesize (*14*). By contrast, *Benwitzia* and *Megaira* exhibit markedly different functional profiles, which may reflect more classical parasitic associations, including sustained ATP parasitism.

Placozoans have emerged as a promising model system for studying metazoan evolution, developmental biology, and tissue formation (*3, 35, 36*). Given their diverse microbiomes and the likely ancestral, widespread, and specific association with *Rickettsiales*, microbial partners should be considered in many research contexts. Most *Rickettsiales* are potent manipulators of host cellular and organismal biology, and the *Midichloriaceae,* with multiple secretion systems and numerous predicted effectors, could influence host development, for instance contributing to arrested early development during sexual reproduction (*10, 14*). At the same time, the intimate integration of intracellular symbionts with host organelles makes placozoans an ideal model for studying host-microbe interactions. Available single-cell atlases from several placozoan lineages (*37*) provide a framework to examine how intracellular *Rickettsiales* stabilize their niches, manipulate hosts, or contribute to host physiology.

358 ## Material & methods

359 **Sample collection, processing and metagenomic and -transcriptomic sequencing**

360 115 individual placozoans were sampled at various field sites (Table S1). Placozoans were identified
361 using a dissection microscope and afterwards kept in culture in 400 ml glass beakers. For individuals
362 kept in culture, the culture medium was 34.5‰ artificial seawater and cultures were fed weekly with
363 $2x10^6$ cells ml^{-1} of *Isochrysis galbana*. Cultures were kept at 25°C and a 16:8 hours light:dark cycle.
364 DNA was extracted from single individuals with the DNeasy Blood & Tissue Kit (Qiagen, Hilden,
365 Germany) according to the manufacturer's instructions with the following exceptions: the proteinase K
366 digest was performed overnight, elution volumes were halved, all samples were eluted twice reusing
367 the first eluate and all elutions were performed after ten minutes of waiting prior to centrifugation.
368 Library construction, quality control and sequencing were performed at the Max Planck Genome
369 Centre (Cologne, Germany). If needed, DNA concentration was increased using the MinElute PCR
370 Purification kit (Qiagen). Libraries for Illumina sequencing were prepared using the Ovation Ultralow
371 Library Systems Kit (NuGEN) according to the manufacturer's instructions or using a miniaturized Tn5
372 transposase-base protocol including a limited PCR step (Table S1). The libraries were size selected by
373 agarose gel electrophoresis. The quality and quantity of selected fragments were analysed by
374 fluorometry and capillary electrophoresis on LabChip GXII Touch. Paired end reads of 100, 150 or
375 250 bp length were sequenced on an Illumina HiSeq 4000 or an Illumina NextSeq 2000 sequences
376 (Table S1). In addition, we included three previously published placozoan metagenomes into our
377 analysis. They were downloaded from the NCBI short read archive (accession numbers SRR5311040,
378 SRR5934055 and SRR5934125).
379
380 Transcriptomes generated from *Trichoplax* sp. H2 from Hawai'i were obtained from ENA (project
381 PRJEB30343). For each transcriptome from *Trichoplax* sp. H2 from Vienna, 20 individuals of a clonal
382 *Trichoplax* sp. H2 strain isolated from a commercial aquarium in Vienna, Austria were processed using
383 the Qiagen RNeasy Micro Kit following the manufacturer's instructions for the isolation of RNA from
384 animal tissue. RNA concentration was determined using the Thermo Fisher Qubit 4.0 with the Qubit RNA
385 High Sensitivity kit. The purified RNA was stored at -80 °C until further processing for RNA sequencing.
386 Samples were processed using the Illumina stranded total RNA kit with Ribozero Plus rRNA depletion
387 (Illumina, San Diego, USA) according to the manufacturer's manual. Sequencing was performed on the
388 NovaSeq 6000 (Illumina, San Diego, USA) using 100bp paired-end sequencing.
389

390 **Assembly of host marker genes, phylogenetic inference and identification of host haplotypes**

391 Mitochondrial 16S rRNA genes of all specimens were assembled by adapting the phyloFlash pipeline
392 to operate on a custom m16S rRNA gene reference database and predict m16S rRNA genes from
393 assembled sequences (*38*). The detected m16S gene sequences were aligned to m16S rRNA gene
394 sequences of previously identified specimens using mafft-xinsi v7.407 (*3, 39–41*). Maximum-likelihood
395 based phylogenies were calculated using IQ-TREE, including automatic selection of the best suited
396 model and generation of 1000 ultrafast bootstrap replicates (*42*). The sequence of *Polyplacotoma*
397 *mediterranea* H0 was used to root the phylogenies. Host haplotypes were defined based on the
398 phylogenetic relations to the previously identified specimens (*3*).
399

400 **Symbiont clade definition and quantification**

401 16S rRNA genes were assembled from the metagenomic libraries using phyloFlash using the –
402 almosteverything option and in addition specifying the read length. All resulting bacterial sequences
403 were inspected for chimera using the uchime algorithm implemented in vsearch v2.6.2 (*43*) and
404 providing sequences matched in the first mapping step of the phyloFlash run as reference database.
405 Only non-chimeric sequences were considered for downstream applications. The reference based on
406 matched sequences from the phyloFlash run was additionally used to place phyloFlash assembled 16S
407 rRNA gene sequences into a phylogenetic tree. The reference database was clustered at 95%

408 sequence identity using the easy_clust algorithm from mmseqs2 (*44*). Assembled sequences and
409 database hits were aligned using mafft-xinsi and a phylogenetic tree was calculated from the resulting
410 alignment using IQ-TREE including automatic selection of the best suited model and generation of 1000
411 ultrafast bootstrap replicates. After verifying the phylogenetic placement, assembled sequences were
412 grouped at the genus-level (for members of the Rickettsiales) or the family level (for all other taxa).
413 The abundances of all groups were quantified across all metagenomic libraries using EMIRGE v.0.61.1
414 following the standard workflow for custom EMIRGE databases (*45*). Chimeric sequences were
415 identified as described above. Additionally, we confirmed phylogenetic placement for non-chimeric
416 sequences by aligning them to the phyloFlash assembled sequences and the clustered collection of
417 phyloFlash database hits using mafft-xinsi and calculating a phylogenetic tree with IQ-TREE (including
418 automatic selection of the best suited model generation of 1000 ultrafast bootstrap replicates).
419 Subsequently, we excluded chimeric sequences, taxa that appear to be contaminations or appeared
420 only once (Note S1, Table S2). After contamination removal, we normalized the relative abundances of
421 the remaining clades to 100%.
422
423 **Phylogeny of all symbionts and their relatives**
424 Sequences of all putative symbiont clades were used to obtain sequences from closely related bacteria
425 from the SILVA database (*46*). Here, we used the SINA search and classify algorithm to obtain up to
426 10 relatives for each sequence that shared at least 90% sequence similarity for each of our input
427 sequences (*47*). For the Rickettsiales, we in addition screened the RefSeq database using BLAST
428 implemented in Geneious v11.1.5 to obtain the ten most similar 16S rRNA genes (*48*). Duplicated
429 sequences were removed from the collection of sequences of the symbionts' relatives. The resulting
430 sequence collection was aligned using mafft-xinsi and a phylogenetic tree was calculated using IQ-
431 TREE including automatic selection of the best suited model generation of 1000 ultrafast bootstrap
432 replicates.
433
434 **Last common ancestor analysis of the *Rickettsiales* symbionts**
435 To determine the evolutionary history of the association of *Rickettsiales* symbionts with placozoans, we
436 performed last common ancestor modeling with pastml (*49*). We used DOWNPASS prediction methods
437 for a maximum-parsimony based estimate.
438
439 **Metagenomic binning and annotation**
440 Symbiont MAGs were generated using a custom pipeline that combines trimming and filtering of raw
441 reads, metagenomic assembly and binning. The exact pipeline is shared under:
442 https://github.com/amankowski/MG-processing_from-reads-to-bins/tree/main. Bin quality was
443 examined by genome completeness and contamination (checkM v1.2.2 (*50*)), the presence of a 16S
444 rRNA gene (barrnap v0.9, https://github.com/tseemann/barrnap) and the number of amino acids that
445 had at least one tRNA encoded in the genome as a second proxy for genome completeness
446 (ARAGORN v1.2.38). Taxonomy was assigned to bins that were of at least medium quality according
447 to MIMAG standards (> 50% complete and showed < 10% contamination, GTDBtk v1.3.0, GTDB r95
448 (*51*, *52*)). If multiple bins were present per library and symbiont taxon, we selected the best one
449 based on genome completeness and contamination estimates, the presence of 16S rRNA, and the
450 number of amino acids with at least one tRNA encoded. We then removed contigs that were shared by
451 at least two bins from the same library. Quality of the final bins of *Rickettsiales* symbionts was checked
452 again with checkM v2 (*53*), barrnap and ARAGORN and the genome statistics of these final bins are
453 reported in Table S4. Functional genome annotations were generated using bakta (*54*). The similarity
454 of metabolism across *Rickettsiales* symbionts was inferred from clusters of orthologous groups (COG)
455 categories, which represent broad functional classifications (*31*). We generated COG category
456 profiles for each symbiont using eggNOG-mapper v2.1.6 (*55*) with DIAMOND alignment (*56*). To
457 quantify functional similarity, we calculated the relative frequencies of COG categories and used them

458 to compute Bray-Curtis distances between genomes. These distances were then visualized using non-
459 metric multidimensional scaling (NMDS). Statistical differences among symbiont taxa were tested using
460 PERMANOVA and ANOSIM with 999 permutations.
461
462 ***Rickettsiales* MAG coverage in sequencing libraries**
463 As an additional measure to assess symbiont presence or absence, we mapped all metagenomic
464 libraries against all MAGs generated in this study. We used coding sequences (CDS) predicted by
465 bakta and read mapping was performed with kallisto v0.45.0 (*57*) with default settings against the
466 full set of predicted CDSs. For each genome, we calculated the proportion of genes to which at least
467 one read mapped, and for *Rickettsiales* genera represented by multiple MAGs, we report the mean
468 proportion across all MAGs.
469
470 **Transcriptome analyses**
471 We quantified transcription levels of ATP synthase and ADP/ATP translocase genes by mapping RNA-
472 seq reads to CDSs of the highest quality *Rickettsiales* reference MAGs from the same host haplotype
473 and sampling location from using kallisto v0.45.0 with default settings.
474
475 **Analyses and plotting of symbiont community composition**
476 The analyses of symbiont community composition were performed in R v4.41 unless differently stated.
477 During the analyses, the following packages were used: (https://github.com/sdray/ade4), tidyverse
478 (*58*), ggplot2 from the tidyverse package,
479 maps (https://www.rdocumentation.org/packages/maps), mapdata
480 (https://www.rdocumentation.org/packages/mapdata).
481
482 **Light and electron microscopy**
483 For light microscopy, placozoan individuals were mounted in artificial sea water (ASW) on glass slides
484 and covered with coverslips for differential interference microscopy using a Leitz Orthoplan light
485 microscope (Leitz, now Leica, Germany) equipped with 25X, 40X and 100X DIC objectives and a
486 Gryphax NAOS 20 MP camera (Jenoptik, Germany). Overview images were recorded using the 25X
487 objective (Air, NA 0.50) and high-magnification images were conducted using the 100X objective (Oil-
488 Immersion, NA 1.30). For electron microscopy, animals were allowed to settle in a type A gold-coated
489 copper sample carrier of 100 µm depth (Leica Microsystems, Germany). Subsequently, ASW was
490 removed, the carrier was filled with 1-hexadecen, sealed with a type B gold-coated copper sample
491 carrier and subjected to high-pressure freezing using a Leica EM ICE (Leica Microsystems, Germany).
492 The frozen samples were placed on top of frozen acetone containing 0.1% osmium tetroxide in liquid
493 nitrogen and freeze substituted (FS) using the Leica AFS2 freeze substitution unit. After 8 hours at -90
494 °C, the temperature was ramped up to -60 °C within 8 hours, held for 8 hours at -60 °C and
495 subsequently ramped up to -40 °C within 4 hours. The samples were incubated for one hour on ice in
496 the FS cocktail, washed with acetone and were infiltrated in Spurr's low viscosity epoxy resin using a
497 fast embedding protocol (*59*).The blocks were cured at 60 °C for 48 hours. Sections were generated
498 using diamond knives (Diatome, Switzerland) on a Leica EM UC7 ultramicrotome (Leica Microsystems,
499 Germany). For light microscopy, 1 µm thin sections were generated that were collect on glass slides
500 and stained with methylene blue. For transmission electron microscopy (TEM), 60 nm ultrathin sections
501 were generated and collected on custom Formvar coated copper slot grids. Before TEM imaging,
502 sections were contrasted 30 minutes with saturated aqueous uranyl acetate (UA) and 1 minute on
503 Reynold's lead citrate. TEM images were recorded using 3a FEI Tecnai G2 Spirit BioTWIN (FEI
504 Company, now Thermo Fisher Scientific, USA) operated at 80 kV or 120 kV.
505
506 **Declaration of generative AI and AI-assisted technologies in the writing process**

During the preparation of this work, the authors used ChatGPT (OpenAI) to improve language and clarity. After the usage of this tool, the authors reviewed and edited the contents as needed and take full responsibility for the content of the article.

Author contributions

AM and HRGV conceived the study and AM analyzed data with input from HRGV and TE. HB generated imaging data of placozoan specimens. HRGV, NL, HN, GN, MGH, and BH acquired placozoan specimens and generated metagenomic data. AM wrote the manuscript together with HRGV and HB, with input from all co-authors.

Declaration of interests

The authors declare no competing interests.

Funding

This work was supported by the Max Planck Society via ND, a Moore Foundation Marine Microbial Initiative Investigator Award to ND (Grant GBMF3811), a DFG Heisenberg Grant (GR 5028/1-1) to HRGV and funding through the DFG CRC 1182 (261376515) to HB.

Availability of data and materials

Raw metagenomic and -transcriptomic sequences are deposited in the European Nucleotide Archive (ENA) under accession ID PRJEB107716 and will be made available upon publication of the manuscript and are currently available upon request. Host and symbiont marker genes as well as symbiont MAGs and annotations are deposited under https://doi.org/10.5281/zenodo.18410361 and will be made available upon publication. We deposited all phylogenetic trees as newick files through iTOL v6 (*60*). Data and scripts used for the generation of figures and statistical analyses are shared under https://github.com/amankowski/placozoan_microbiome.

Acknowledgements

We are thankful for sample collections and field assistance by Chris Keller, Daniel Abed-Navandi, Emilia M. Sogin, Laetitia Wilkins, Ramon Rossello-Mora, Tomas Wilkop and Zach Foltz. In addition, we would like to thank the Carrie Bow Cay Laboratory and the Bocas del Toro Research Station of the Smithsonian Tropical Research Institute, the Haus des Meeres Vienna, the Las Palma Aquarium and their staff for supporting our sampling campaigns. We thank Sam Vohsen for constructive scientific discussions. We also thank the Central Microscopy (Kiel University) for their support with TEM acquisition (Urska Repnik). This work is contribution XXX from the Carrie Bow Cay Laboratory, Caribbean Coral Reef Ecosystem Program, National Museum of History, Washington DC.

References

1. A. C. Darby, N. H. Cho, H. H. Fuxelius, J. Westberg, S. G. E. Andersson (2007) Intracellular pathogens go extreme: genome evolution in the Rickettsiales. Trends Genet **23**, 511-520.
2. J. Salje (2001) Cells within cells: Rickettsiales and the obligate intracellular bacterial lifestyle. Nat Rev Microbiol **19**, 375-390.
3. M. Eitel, H.-J. Osigus, R. DeSalle, B. Schierwater (2013) Global Diversity of the Placozoa. *PLoS One* **8**, e57131.
4. P. Simion, H. Philippe, D. Baurain, M. Jager, D. J. Richter, A. Di Franco, B. Roure, N. Satoh, É. Quéinnec, A. Ereskovsky, P. Lapébie, E. Corre, F. Delsuc, N. King, G. Wörheide, M. Manuel, A (2017) Large and Consistent Phylogenomic Dataset Supports Sponges as the Sister Group to All Other Animals. *Curr Biol* **27**, 958–967.
5. C. E. Laumer, H. Gruber-Vodicka, M. G. Hadfield, V. B. Pearse, A. Riesgo, J. C. Marioni, G. Giribet (2018) Support for a clade of Placozoa and Cnidaria in genes with minimal compositional bias. *Elife* **7**, e36278.
6. M. Eitel, W. R. Francis, F. Varoqueaux, J. Daraspe, H.-J. Osigus, S. Krebs, S. Vargas, H. Blum, G. A. Williams, B. Schierwater, G. Wörheide (2018) Comparative genomics and the nature of placozoan species. *PLoS Biol* **16**, e2005359.

7. F. E. Schulze (1883) Trichoplax adhaerens, nov. gen., nov. spec. *Zool Anz* **6**, 92–97.
8. H.-J. Osigus, S. Rolfes, R. Herzog, K. Kamm, B. Schierwater (2019) *Polyplacotoma mediterranea* is a new ramified placozoan species. *Curr Biol* **29**, R148–R149.
9. K. G. Grell, G. Benwitz (1971) Die ultrastruktur von *Trichoplax adhaerens* F.E. Schulze. *Cytobiologie* **4**, 216–240.
10. M. Eitel, L. Guidi, H. Hadrys, M. Balsamo, B. Schierwater (2011) New insights into placozoan sexual reproduction and development. *PLoS One* **6** e19639.
11. L. Guidi, M. Eitel, E. Cesarini, B. Schierwater, M. Balsamo (2011) Ultrastructural analyses support different morphological lineages in the phylum placozoa Grell, 1971. *J Morphol* **272**, 371–378.
12. C. L. Smith, F. Varoqueaux, M. Kittelmann, R. N. Azzam, B. Cooper, C. A. Winters, M. Eitel, D. Fasshauer, T. S. Reese (2014) Novel Cell Types, Neurosecretory Cells, and Body Plan of the Early-Diverging Metazoan *Trichoplax adhaerens* Curr *Biol* **24**, 1565–1572.
13. J. G. Klinges, S. M. Rosales, R. McMinds, E. C. Shaver, A. A. Shantz, E. C. Peters, M. Eitel, G. Wörheide, K. H. Sharp, D. E. Burkepile, B. R. Silliman, R. L. Vega Thurber (2019) Phylogenetic, genomic, and biogeographic characterization of a novel and ubiquitous marine invertebrate-associated Rickettsiales parasite, Candidatus Aquarickettsia rohweri, gen. nov., sp. nov. *ISME J.* **13**, 2938–2953.
14. H. R. Gruber-Vodicka, N. Leisch, M. Kleiner, T. Hinzke, M. Liebeke, M. McFall-Ngai, M. G. Hadfield, N. Dubilier (2019) Two intracellular and cell type-specific bacterial symbionts in the placozoan Trichoplax H2. *Nat Microbiol* **4**, 1465–1474.
15. T. Driscoll, J. J. Gillespie, E. K. Nordberg, A. F. Azad, B. W. Sobral (2013) Bacterial DNA Sifted from the Trichoplax adhaerens (Animalia: Placozoa) Genome Project Reveals a Putative Rickettsial Endosymbiont. *Genome Biol Evol* **5**, 621–645.
16. K. Kamm, H. J. Osigus, P. F. Stadler, R. DeSalle, B. Schierwater (2019) Genome analyses of a placozoan rickettsial endosymbiont show a combination of mutualistic and parasitic traits. *Sci Rep* **9** 17561.
17. M. Tessler, J. S. Neumann, K. Kamm, H. J. Osigus, G. Eshel, A. Narechania, J. A. Burns, R. DeSalle, B. Schierwater (2022) Phylogenomics and the first higher taxonomy of Placozoa, an ancient and enigmatic animal phylum. *Front Ecol Evol* **10** .
18. L. J. Baker, H. G. Reich, S. A. Kitchen, J. Grace Klinges, H. R. Koch, I. B. Baums, E. M. Muller, R. V. Thurber (2022) The coral symbiont Candidatus Aquarickettsia is variably abundant in threatened Caribbean acroporids and transmitted horizontally. *ISME J* **16**, 400–411.
19. B. Schierwater, H.-J. Osigus, T. Bergmann, N. W. Blackstone, H. Hadrys, J. Hauslage, P. O. Humbert, K. Kamm, M. Kvansakul, K. Wysocki, R. DeSalle (2021)The enigmatic Placozoa part 1: Exploring evolutionary controversies and poor ecological knowledge. *BioEssays* **43**, 2100080.
20. O. Duron, P. Doublet, F. Vavre, D. Bouchon (2018) The Importance of Revisiting Legionellales Diversity. *Trends Parasitol* **34**, 1027–1037.
21. M. Horn (2008) Chlamydiae as Symbionts in Eukaryotes. *Annu Rev Microbiol* **62**, 113–131.
22. C. Hochart, L. Paoli, H. J. Ruscheweyh, G. Salazar, E. Boissin, S. Romac, J. Poulain, G. Bourdin, G. Iwankow, C. Moulin, M. Ziegler, B. Porro, E. J. Armstrong, B. C. C. Hume, J. M. Aury, C. Pogoreutz, D. A. Paz-García, M. M. Nugues, S. Agostini, B. Banaigs, E. Boss, C. Bowler, C. de Vargas, E. Douville, M. Flores, D. Forcioli, P. Furla, E. Gilson, F. Lombard, S. Pesant, S. Reynaud, O. P. Thomas, R. Troublé, P. Wincker, D. Zoccola, D. Allemand, S. Planes, R. V. Thurber, C. R. Voolstra, S. Sunagawa, P. E. Galand (2023) Ecology of Endozoicomonadaceae in three coral genera across the Pacific Ocean. *Nat Commun* **14** 3037.
23. M. Á. G. Porras, A. Assié, M. Tietjen, M. Violette, M. Kleiner, H. Gruber-Vodicka, N. Dubilier, N. Leisch (2024) An intranuclear bacterial parasite of deep-sea mussels expresses apoptosis inhibitors acquired from its host. *Nat Microbiol* **9** 2877-2891.
24. J. O. Bartz, J. Blom, H. J. Busse, J. B. Mvie, M. Hardt, P. Schubert, T. Wilke, A. Goessmann, G. Wilharm, J. Bender, P. Kämpfer, S. P. Glaeser (2018) Parendozoicomonas haliclonae gen. nov. sp. nov. isolated from a marine sponge of the genus Haliclona and description of the family Endozoicomonadaceae fam. nov. comprising the genera Endozoicomonas, Parendozoicomonas, and Kistimonas. *Syst Appl Microbiol* **41**, 73–84.
25. E. E. George, D. Barcytė, G. Lax, S. Livingston, D. Tashyreva, F. Husnik, J. Lukeš, M. Eliáš, P. J. Keeling (2023) A single cryptomonad cell harbors a complex community of organelles, bacteria, a phage, and selfish elements. *Curr Biol* **33**, 1982-1996.e4.
26. D. Giannotti, V. Boscaro, F. Husnik, C. Vannini, P. J. Keeling (2022) The "Other" Rickettsiales: an Overview of the Family "Candidatus Midichloriaceae". *Appl Environ Microbiol* **88**, e02432-21.
27. V. Boscaro, F. Husnik, C. Vannini, P. J. Keeling (2019) Symbionts of the ciliate *Euplotes*: diversity, patterns and potential as models for bacteria–eukaryote endosymbioses. *Proc Biol Sci* **286**, 1–10 (2019).
28. K. G. Grell, G. Benwitz (1981) Ergänzende Untersuchungen zur Ultrastruktur von Trichoplax adhaerens F.E. Schulze (Placozoa). *Zoomorphology* **98**, 47–67.
29. T. D. Mayorova, K. Hammar, C. A. Winters, T. S. Reese, C. L. Smith (2019) The ventral epithelium of Trichoplax adhaerens deploys in distinct patterns cells that secrete digestive enzymes, mucus or diverse neuropeptides. *Biol Open* **8**, bio045674.
30. D. Y. Romanova, F. Varoqueaux, J. Daraspe, M. A. Nikitin, M. Eitel, D. Fasshauer, L. L. Moroz (2021) Hidden cell diversity in Placozoa: ultrastructural insights from Hoilungia hongkongensis. *Cell Tissue Res* **385**, 623–637.
31. R. L. Tatusov, E. V Koonin, D. J. Lipman (1997) A Genomic Perspective on Protein Families. *Science (1979)*. **278**, 631–637.
32. T. P. Driscoll., V. I. Verhoeve., M. L. Guilotte, S. S. Lehman, S. A. Rennoll, M. Beier-Sexton, M. Sayeedur Rahman, A. F. Azad, J. J. Gillespie (2017) Wholly Rickettsia! Reconstructed Metabolic Profile of the Quintessential Bacterial Parasite of Eukaryotic Cells. *mBio* **8**, e00859-17.
33. S. Schmitz-Esser, N. Linka, A. Collingro, C. L. Beier, H. E. Neuhaus, M. Wagner, M. Horn (2004) ATP/ADP Translocases: A Common Feature of Obligate Intracellular Amoebal Symbionts Related to Chlamydiae and Rickettsiae *J. Bacteriol* **186**, 683–691.

34. M. E. Schön, J. Martijn, J. Vosseberg, S. Köstlbacher, T. J. G. Ettema (2022) The evolutionary origin of host association in the Rickettsiales. *Nat Microbiol* **7**, 1189–1199.
35. A. Sebé-Pedrós, E. Chomsky, K. Pang, D. Lara-Astiaso, F. Gaiti, Z. Mukamel, I. Amit, A. Hejnol, B. M. Degnan, A. Tanay (2018) Early metazoan cell type diversity and the evolution of multicellular gene regulation. *Nat Ecol Evol* **2**, 1176–1188.
36. M. Srivastava, E. Begovic, J. Chapman, N. H. Putnam, U. Hellsten, T. Kawashima, A. Kuo, T. Mitros, A. Salamov, M. L. Carpenter, A. Y. Signorovitch, M. A. Moreno, K. Kamm, J. Grimwood, J. Schmutz, H. Shapiro, I. V Grigoriev, L. W. Buss, B. Schierwater, S. L. Dellaporta, D. S. Rokhsar (2008) The Trichoplax genome and the nature of placozoans. *Nature* **454**, 955–960.
37. S. R. Najle, X. Grau-Bové, A. Elek, C. Navarrete, D. Cianferoni, C. Chiva, D. Cañas-Armenteros, A. Mallabiabarrena, K. Kamm, E. Sabidó, H. Gruber-Vodicka, B. Schierwater, L. Serrano, A. Sebé-Pedrós (2023) Stepwise emergence of the neuronal gene expression program in early animal evolution. *Cell* **186**, 4676-4693.e2.
38. H. R. Gruber-Vodicka, B. K. B. Seah, E. Pruesse (2020) phyloFlash: Rapid Small-Subunit rRNA Profiling and Targeted Assembly from Metagenomes. *mSystems* **5**, e00920-20.
39. K. Katoh, K. Kuma, H. Toh, T. Miyata (2005) MAFFT version 5: improvement in accuracy of multiple sequence alignment. *Nucleic Acids Res* **33**, 511–518.
40. K. Katoh, D. M. Standley (2013) MAFFT Multiple Sequence Alignment Software Version 7: Improvements in Performance and Usability. *Mol Biol Evol* **30**, 772–780.
41. K. Katoh, K. Misawa, K. Kuma, T. Miyata (2022) MAFFT: a novel method for rapid multiple sequence alignment based on fast Fourier transform. *Nucleic Acids Res* **30**, 3059–3066.
42. L.-T. Nguyen, H. A. Schmidt, A. von Haeseler, B. Q. Minh (2015) IQ-TREE: A Fast and Effective Stochastic Algorithm for Estimating Maximum-Likelihood Phylogenies. *Mol Biol Evol* **32**, 268–274.
43. T. Rognes, T. Flouri, B. Nichols, C. Quince, F. Mahé (2016) VSEARCH: a versatile open source tool for metagenomics. *PeerJ* **4**, e2584.
44. M. Steinegger, J. Söding (2017) MMseqs2 enables sensitive protein sequence searching for the analysis of massive data sets. *Nat Biotechnol* **35**, 1026–1028.
45. C. S. Miller, B. J. Baker, B. C. Thomas, J. F. Singer Steven W. & Banfield (2011) EMIRGE: reconstruction of full-length ribosomal genes from microbial community short read sequencing data. *Genome Biol* **12**, R44.
46. P. Yilmaz, L. W. Parfrey, P. Yarza, J. Gerken, E. Pruesse, C. Quast, T. Schweer, J. Peplies, W. Ludwig, F. O. Glöckner (2014) The SILVA and "All-species Living Tree Project (LTP)" taxonomic frameworks. *Nucleic Acids Res* **42**, D643–D648.
47. C. Quast, E. Pruesse, P. Yilmaz, J. Gerken, T. Schweer, P. Yarza, J. Peplies, F. O. Glockner (2013) The SILVA ribosomal RNA gene database project: improved data processing and web-based tools. *Nucleic Acids Res* **41**, D590--6.
48. S. F. Altschul, W. Gish, W. Miller, D. J. Myers E. W. & Lipman (1990) Basic local alignment search tool. *J Mol Biol* **215**, 403–410.
49. S. A. Ishikawa, A. Zhukova, W. Iwasaki, O. Gascuel (2019) A Fast Likelihood Method to Reconstruct and Visualize Ancestral Scenarios. *Mol Biol Evol* **36**, 2069–2085.
50. D. H. Parks, M. Imelfort, C. T. Skennerton, G. W. Hugenholtz Philip & Tyson (2015) CheckM: assessing the quality of microbial genomes recovered from isolates, single cells, and metagenomes. *Genome Res* **25**, 1043–1055.
51. P.-A. Chaumeil, A. J. Mussig, P. Hugenholtz, D. H. Parks (2020) GTDB-Tk: a toolkit to classify genomes with the Genome Taxonomy Database. *Bioinformatics* **36**, 1925–1927.
52. D. H. Parks, M. Chuvochina, C. Rinke, A. J. Mussig, P.-A. Chaumeil, P. Hugenholtz (2022) GTDB: an ongoing census of bacterial and archaeal diversity through a phylogenetically consistent, rank normalized and complete genome-based taxonomy. *Nucleic Acids Res.* **50**, D785–D794.
53. A. Chklovski, D. H. Parks, B. J. Woodcroft, G. W. Tyson (2023) CheckM2: a rapid, scalable and accurate tool for assessing microbial genome quality using machine learning. *Nat Methods* **20**, 1203–1212.
54. O. Schwengers, L. Jelonek, M. A. Dieckmann, S. Beyvers, J. Blom, A. Goesmann (2021) Bakta: rapid and standardized annotation of bacterial genomes via alignment-free sequence identification. *Microb Genom* **7** 685.
55. C. P. Cantalapiedra, A. Hernández-Plaza, I. Letunic, P. Bork, J. Huerta-Cepas (2021) eggNOG-mapper v2: Functional Annotation, Orthology Assignments, and Domain Prediction at the Metagenomic Scale. *Mol Biol Evol* **38**, 5825–5829.
56. B. Buchfink, C. Xie, D. H. Huson, Fast and sensitive protein alignment using DIAMOND. *Nat. Methods* **12**, 59–60.
57. N. L. Bray, H. Pimentel, P. Melsted, L. Pachter (2015) Near-optimal probabilistic RNA-seq quantification. *Nat Biotechnol* **34**, 525–527 (2016).
58. H. Wickham, M. Averick, J. Bryan, W. Chang, L. D. McGowan, R. François, G. Grolemund, A. Hayes, L. Henry, J. Hester, M. Kuhn, T. L. Pedersen, E. Miller, S. M. Bache, K. Müller, J. Ooms, D. Robinson, D. P. Seidel, V. Spinu, K. Takahashi, D. Vaughan, C. Wilke, K. Woo, H. Yutani (2019) Welcome to the Tidyverse. *J. Open Source Softw.* **4**, 1686.
59. K. L. McDonald (2014) Rapid Embedding Methods into Epoxy and LR White Resins for Morphological and Immunological Analysis of Cryofixed Biological Specimens. *Microscopy and Microanalysis* **20**, 152–163.
60. I. Letunic, P. Bork (2024) Interactive Tree of Life (iTOL) v6: Recent updates to the phylogenetic tree display and annotation tool. *Nucleic Acids Res.* **52**, W78–W82.
61. A. M. Jackson, L. W. Buss (2009) Shiny spheres of placozoans (Trichoplax) function in anti-predator defense. *Invertebrate Biology* **128**, 205–212.
62. T. D. Mayorova, C. L. Smith, K. Hammar, C. A. Winters, N. B. Pivovarova, M. A. Aronova, R. D. Leapman, T. S. Reese (2018) Cells containing aragonite crystals mediate responses to gravity in Trichoplax adhaerens (Placozoa), an animal lacking neurons and synapses. *PLoS One* **13**, e0190905.
63. R. Cuervo-González (2017) Rhodope placozophagus (Heterobranchia) a new species of turbellarian-like Gastropoda that preys on placozoans. *Zool. Anz.* **270**, 43–48.